Inorg. Chem. **2005**, *44*, 2659–2665

The Satellite-Shaped Co-15 Polyoxotungstate, $[Co_6(H_2O)_{30}\{Co_9Cl_2(OH)_3(H_2O)_9(\beta\text{-}SiW_8O_{31})_3\}]^{5-}$

Bassem S. Bassil,[†] Saritha Nellutla,[‡] Ulrich Kortz,*[,†] Ashley C. Stowe,[‡] Johan van Tol, Naresh S. Dalal,*[,‡] Bineta Keita,[§] and Louis Nadjo*[,§]

School of Engineering and Science, International University Bremen, P.O. Box 750 561, 28725 Bremen, Germany, Department of Chemistry and Biochemistry, Florida State University and National High Magnetic Field Laboratory and Center for Interdisciplinary Magnetic Resonance, Tallahassee, Florida 32306-4390, and Laboratoire de Chimie Physique, UMR 8000, CNRS, Equipe d'Electrochimie et Photoélectrochimie, Université Paris-Sud, Bâtiment 420, 91405 Orsay Cedex, France

Received December 9, 2004

The 15-cobalt-substituted polyoxotungstate $[Co_6(H_2O)_{30}\{Co_9Cl_2(OH)_3(H_2O)_9(\beta\text{-}SiW_8O_{31})_3\}]^{5-}$ (**1**) has been characterized by single-crystal XRD, elemental analysis, IR, electrochemistry, magnetic measurements, and EPR. Single-crystal X-ray analysis was carried out on $Na_5[Co_6(H_2O)_{30}\{Co_9Cl_2(OH)_3(H_2O)_9(\beta\text{-}SiW_8O_{31})_3\}]\cdot 37H_2O$, which crystallizes in the hexagonal system, space group $P6_3/m$, with $a = 19.8754(17)$ Å, $b = 19.8754(17)$ Å, $c = 22.344(4)$ Å, $\alpha = 90°$, $\beta = 90°$, $\gamma = 120°$, and $Z = 2$. The trimeric polyanion **1** has a core of nine Co^{II} ions encapsulated by three unprecedented (β-SiW_8O_{31}) fragments and two Cl^- ligands. This central assembly $\{Co_9Cl_2(OH)_3(H_2O)_9(\beta\text{-}SiW_8O_{31})_3\}^{17-}$ is surrounded by six antenna-like $Co^{II}(H_2O)_5$ groups resulting in the satellite-like structure **1**. Synthesis of **1** is accomplished in a simple one-pot procedure by interaction of Co^{II} ions with $[\gamma\text{-}SiW_{10}O_{36}]^{8-}$ in aqueous, acidic NaCl medium (pH 5.4). Polyanion **1** was studied by cyclic voltammetry as a function of pH. The current intensity of its Co^{II} centers was compared with that of free Co^{II} in solution. Our results suggest that **1** keeps its integrity in solution. Magnetic susceptibility results show the presence of both antiferro- and ferromagnetic coupling within the $(Co^{II})_9$ core. A fully anisotropic Ising model has been employed to describe the exchange-coupling and yields $g = 2.42 \pm 0.01$, $J_1 = 17.0 \pm 1.5$ cm^{-1}, and $J_2 = -13 \pm 1$ cm^{-1}. Variable frequency EPR studies reveal an anisotropic Kramer's doublet.

Introduction

Polyoxometalates (POMs) are a well-known class of metal−oxygen clusters with an unmatched structural variety combined with a multitude of properties.[1,2] The first POM was identified in the early 19th century, but its structure could not be revealed until a century later.[3,4] The search for novel POMs is predominantly driven by the exciting catalytic, medicinal, and magnetic properties of many transition metal substituted polyoxotungstates. For example, the catalytic activity of POMs (e.g., oxidation) combined with high thermal stability have led to industrial applications of these species, mostly as heterogeneous catalysts in the oxidation of organic substrates.[2b,d,e,f] Transition metal substituted polyoxotungstates can also be of interest for their magnetic properties.[2b,d,e,f] Structures that contain more than one

* Author to whom correspondence should be addressed. E-mail: u.kortz@iu-bremen.de. Fax: (+49)421-200-3229.
[†] International University Bremen.
[‡] Florida State University and National High Magnetic Field Laboratory and Center for Interdisciplinary Magnetic Resonance.
[§] Université Paris-Sud.

(1) Pope, M. T. *Heteropoly and Isopoly Oxometalates;* Springer: Berlin, 1983.
(2) (a) Pope, M. T.; Müller, A. *Angew. Chem., Int. Ed. Engl.* **1991**, *30*, 34. (b) Pope, M. T., Müller, A., Eds. *Polyoxometalates*: *From Platonic Solids to Anti Retroviral Activity*; Kluwer: Dordrecht, 1994. (c) Hill, C. L.; Prosser-McCartha, C. M. *Coord. Chem. Rev.* **1995**, *143*, 407. (d) *Chem. Rev.* **1998**, *98*, 1−389 (Special Thematic Issue on Polyoxometalates). (e) Pope, M. T., Müller, A., Eds. *Polyoxometalate Chemistry*: *From Topology via Self-Assembly to Applications*; Kluwer: Dordrecht, 2001. (f) Yamase, T., Pope, M. T., Eds. *Polyoxometalate Chemistry for Nano-Composite Design*; Kluwer: Dordrecht, 2002. (g) Pope, M. T. *Comput. Coord. Chem. II* **2003**, *4*, 635. (h) Hill, C. L. *Comput. Coord. Chem. II* **2003**, *4*, 679. (i) Borrás-Almenar, J. J., Coronado, E., Müller, A., Pope, M. T., Eds. *Polyoxometalate Molecular Science*; Kluwer: Dordrecht, 2004.
(3) Berzelius, J. *Pogg. Ann.* **1826**, *6*, 369.
(4) (a) Keggin, J. F. *Nature* **1933**, *131*, 908. (b) Keggin, J. F. *Proc. R. Soc. London, Ser. A* **1934**, *144*, 75.

10.1021/ic048269x CCC: $30.25
Published on Web 03/22/2005

paramagnetic transition metal ion in close proximity may exhibit exchange-coupled spins leading to large spin ground states.

However, the discovery of novel, discrete POMs is complicated by the fact that the mechanism of formation of POMs is not well understood and commonly described as self-assembly. A common synthetic strategy for the preparation of transition metal substituted polyoxotungstates involves reaction of a transition metal ion with a lacunary POM. The tungsten-oxo framework is usually preserved in the product, if a stable lacunary POM is used (e.g., α-$PW_{11}O_{39}^{7-}$, $P_2W_{15}O_{56}^{12-}$, *A*-$SiW_9O_{34}^{10-}$).[1]

Our group has shown that this is not the case for the divacant decatungstosilicate, $[\gamma\text{-}SiW_{10}O_{36}]^{8-}$, which was first reported by Hervé and co-workers.[5] Reaction of $[\gamma\text{-}SiW_{10}O_{36}]^{8-}$ with a variety of first-row transition metals has led to dimeric ($[\{\beta\text{-}SiNi_2W_{10}O_{36}(OH)_2(H_2O)\}_2]^{12-}$, $[M_4(H_2O)_2(B\text{-}\alpha\text{-}GeW_9O_{34})_2]^{12-}$ (M = Mn^{2+}, Cu^{2+}, Zn^{2+}, Cd^{2+})), trimeric ($[(\beta_2\text{-}SiW_{11}MnO_{38}OH)_3]^{15-}$), and tetrameric ($[\{\beta\text{-}Ti_2SiW_{10}O_{39}\}_4]^{24-}$) products, and in all cases the γ-tungsten-oxo framework was not preserved.[6−9] We can conclude that the dilacunary precursor $[\gamma\text{-}SiW_{10}O_{36}]^{8-}$ isomerizes easily in aqueous, acidic medium upon heating and in the presence of first-row transition metal ions, which can result in oligomeric products with unexpected structures. Therefore, we decided to investigate the system $Co^{II}/[\gamma\text{-}SiW_{10}O_{36}]^{8-}$ in some detail.

Experimental Section

Synthesis. All reagents were used as purchased without further purification. The dilacunary precursor $K_8[\gamma\text{-}SiW_{10}O_{36}]$ was synthesized according to the published procedure.[10]

$Na_5[Co_6(H_2O)_{30}\{Co_9Cl_2(OH)_3(H_2O)_9(\beta\text{-}SiW_8O_{31})_3\}]\cdot 37H_2O$ (Na_5-1). A 1.00 g (0.36 mmol) sample of $K_8[\gamma\text{-}SiW_{10}O_{36}]$ was added with stirring to a solution of 1.14 g (4.75 mmol) of $CoCl_2\cdot 6H_2O$ in 20 mL of 1 M NaCl. After complete dissolution (~5 min), the pH was adjusted to 5.5 by addition of 0.1 M NaOH. This solution was heated to 50 °C for 30 min and then cooled to room temperature and filtered. Slow evaporation at room temperature resulted in a purple/red crystalline product after 2−3 days that was filtered off and air-dried. Yield: 0.66 g (65%). IR: 995(m), 937(s), 891(sh), 852(s), 804(m), 750(sh), 695(s), 554(w), 534(w), 496(w) cm^{-1}. Anal. Calcd for **Na_5-1**: Na, 1.4; W, 52.1; Co, 10.4; Si, 1.0; Cl, 0.8. Found: Na, 1.4; W, 53.0; Co, 10.0; Si, 1.1; Cl, 0.9. Elemental analysis was performed by Kanti Labs Ltd. in Mississauga, Canada.

X-ray Crystallography. A red block of **Na_5-1** with dimensions $0.15 \times 0.05 \times 0.03$ mm^3 was mounted on a glass fiber for indexing and intensity data collection at 200 K on a Bruker D8 SMART APEX CCD single-crystal diffractometer using Mo Kα radiation ($\lambda = 0.71073$ Å). Of the 6502 unique reflections ($2\theta_{max} = 56.66°$), 6173 reflections ($R_{int} = 0.132$) were considered observed ($I > 2\sigma(I)$). Direct methods were used to solve the structure and to locate the tungsten and cobalt atoms (SHELXS-97). Then the remaining atoms were found from successive difference maps (SHELXL-97). The final cycle of refinement, including the atomic coordinates, anisotropic thermal parameters (W, Co, Si, Na, and Cl atoms), and isotropic thermal parameters (O atoms) converged at $R = 0.081$ and $R_w = 0.150$ ($I > 2\sigma(I)$). In the final difference map the deepest hole was −3.359 eÅ^{-3} and the highest peak was 5.603 eÅ^{-3}. Routine Lorentz and polarization corrections were applied and an absorption correction was performed using the SADABS program.[11] Crystallographic data are summarized in Table 1.

Table 1. Crystal Data and Structure Refinement for $Na_5[Co_6(H_2O)_{30}\{Co_9Cl_2(OH)_3(H_2O)_9(\beta\text{-}SiW_8O_{31})_3\}]\cdot 37H_2O$ (**Na_5-1**)

emp formula	$Cl_2Co_{15}H_{155}Na_5O_{172}Si_3W_{24}$
fw	8475.2
space group (No.)	$P6_3/m$ (176)
a (Å)	19.8754(17)
b (Å)	19.8754(17)
c (Å)	22.344(4)
α (°)	90
β (°)	90
γ (°)	120
vol (Å^3)	7643.9(16)
Z	2
temp (°C)	−73
wavelength (Å)	0.71073
d_{calcd} (mg m^{-3})	3.622
abs coeff (mm^{-1})	19.752
R [$I > 2\sigma(I)$][a]	0.081
R_w (all data)[b]	0.150

[a] $R = \sum||F_o| - |F_c||/\sum|F_o|$. [b] $R_w = [\sum w(F_o^2 - F_c^2)^2/\sum w(F_o^2)^2]^{1/2}$.

UV−Visible Spectroscopy. Pure water was used throughout. It was obtained by passing through a RiOs 8 unit followed by a Millipore-Q Academic purification set. All reagents were of high-purity grade and were used as purchased without further purification. The UV−visible spectra were recorded on a Perkin-Elmer Lambda 19 spectrophotometer on 1.6×10^{-5} M solutions of the relevant polyanion. Matched 1.000 cm optical path quartz cuvettes were used. The compositions of the various media were as follows: for pH 0.27: 1 M HCl: for pH 3: 1 M LiCl + HCl + 0.069 M PHP (potassium hydrogen phthalate).

Electrochemistry. The same media as for UV−visible spectroscopy were used for electrochemistry, but the polyanion concentration was 2×10^{-4} M. The solutions were deaerated thoroughly for at least 30 min. with pure argon and kept under a positive pressure of this gas during the experiments. The source, mounting, and polishing of the glassy carbon (GC, Tokai, Japan) electrodes has been described.[12] The glassy carbon samples had a diameter of 3 mm. The electrochemical setup was an EG & G 273 A driven by a PC with the M270 software. Potentials are quoted against a saturated calomel electrode (SCE). The counter electrode was a platinum gauze of large surface area. All experiments were performed at room temperature.

Magnetic and EPR Measurements. Magnetic measurements on powder samples of **Na_5-1** were carried out using a Quantum Design MPMS-XL SQUID magnetometer over the temperature range 1.8−300 K up to 7 T. Data were corrected for diamagnetism (-3.0×10^{-3} emu/mol) using Klemm constants[13] and TIP (1.5×10^{-4} emu/mol per Co^{II} ion) reported by Casañ-Pastor et al.[14]

(5) Canny, J.; Tézé, A.; Thouvenot, R.; Hervé, G. *Inorg. Chem.* **1986**, *25*, 2114.
(6) Kortz, U.; Jeannin, Y. P.; Tézé, A.; Hervé, G.; Isber, S. *Inorg. Chem.* **1999**, *38*, 3670.
(7) Kortz, U.; Isber, S.; Dickman, M. H.; Ravot, D. *Inorg. Chem.* **2000**, *39*, 2915.
(8) Kortz, U.; Matta, S. *Inorg. Chem.* **2001**, *40*, 815.
(9) Hussain, F.; Bassil, B. S.; Bi, L.-H.; Reicke, M.; Kortz, U. *Angew. Chem., Int. Ed.* **2004**, *43*, 3485.
(10) Tézé, A.; Hervé, A., G. *Inorg. Syntheses* **1990**, *27*, 88.
(11) Sheldrick, G. M. Siemens Analytical X-ray Instrument Division: Madison, WI, 1995.
(12) Keita, B.; Girard, F.; Nadjo, L.; Contant, R.; Belghiche, R.; Abbessi, M. *J. Electroanal. Chem.* **2001**, *508*, 70.
(13) Vulfson, S. G. *Molecular Magnetochemistry*; Gordon and Breach Science: Newark, NJ, 1998.

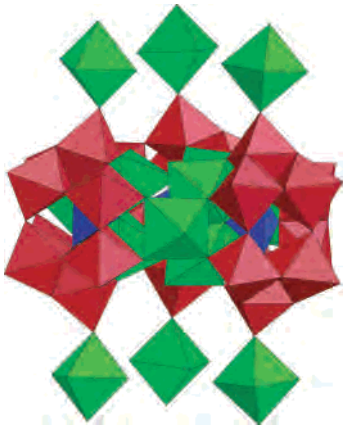

Figure 1. Polyhedral representation (side view) of $[Co_6(H_2O)_{30}\{Co_9Cl_2(OH)_3(H_2O)_9(\beta\text{-}SiW_8O_{31})_3\}]^{5-}$ (**1**). The polyhedra represent WO_6 (red), CoO_6 (green), and SiO_4 (blue).

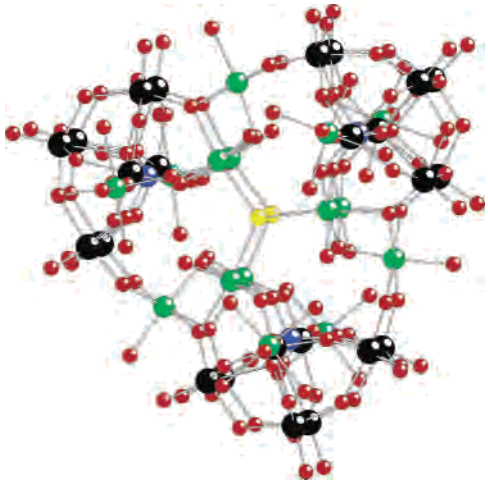

Figure 2. Ball and stick representation (top view) of $[Co_6(H_2O)_{30}\{Co_9Cl_2(OH)_3(H_2O)_9(\beta\text{-}SiW_8O_{31})_3\}]^{5-}$ (**1**). The color code is as follows: tungsten (black), cobalt (green), silicon (blue), oxygen (red), and chlorine (yellow).

Polycrystalline powder EPR spectra of **Na_5-1** were recorded using a Bruker Elexsys-500 spectrometer at Q-band (~34 GHz) in the temperature range 4−300 K. High-frequency EPR experiments were conducted on a custom-built variable frequency EPR spectrometer at the National High Magnetic Field Laboratory in Tallahassee.[15]

Results and Discussion

Synthesis and Structure. Interaction of Co^{II} ions with $[\gamma\text{-}SiW_{10}O_{36}]^{8-}$ in the ratio 12:1 in a 1 M NaCl medium (pH adjusted to 5.4) resulted in the novel, trimeric $[Co_6(H_2O)_{30}\{Co_9Cl_2(OH)_3(H_2O)_9(\beta\text{-}SiW_8O_{31})_3\}]^{5-}$ (**1**), see Figures 1 and 2. The core of polyanion **1** is composed of nine Co^{II} ions that are encapsulated by three unprecedented (β-SiW_8O_{31}) fragments and two Cl^- ligands (see Figure 3). This central assembly $\{Co_9Cl_2(OH)_3(H_2O)_9(\beta\text{-}SiW_8O_{31})_3\}^{17-}$ is surrounded by six antenna-like $Co^{II}(H_2O)_5$ groups, which are bound to terminal oxo groups, resulting in the title polyanion

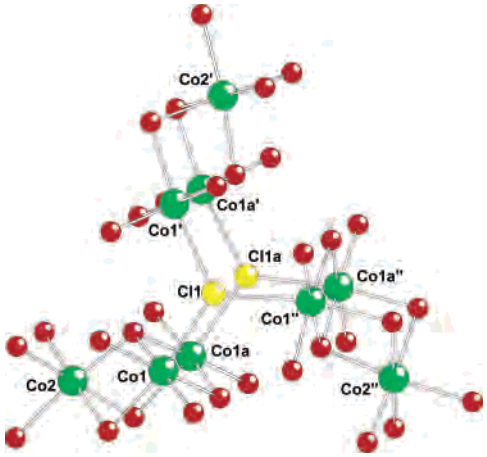

Figure 3. Ball and stick representation (top view) of the central cobalt-oxo fragment in $[Co_6(H_2O)_{30}\{Co_9Cl_2(OH)_3(H_2O)_9(\beta\text{-}SiW_8O_{31})_3\}]^{5-}$ (**1**). The color code is the same as in Figure 2.

1. Three of these antenna are each above and below **1**, so that the structure of the title polyanion could be described as satellite-like.

We believe that the six "outer" Co^{II} ions play an important stabilizing role by reducing the charge of the core of **1** by 12 units from −17 to −5. The six capping Co^{II} ions are attached via one covalent bond to the core of **1** (Co3−O2T 2.07(1) Å, W2−O2T 1.75(1) Å). On the basis of structural arguments we believe that the core of **1** could also exist independently, without the six outer cobalt ions. In this case charge compensation could perhaps be achieved by protons or tightly bound alkali counterions (e.g., K^+). Alternatively, substitution of the nine "inner" Co^{II} ions by high-valent, early transition metal ions (e.g., Ti^{IV}, Zr^{IV}, V^V, and Mo^{VI}) might lead to stable derivatives of **1**.

The title polyanion **1** represents only the second example of a structurally characterized cobalt-substituted tungstosilicate.[16] Furthermore, **1** contains more paramagnetic transition metal centers than any other polyoxotungstate known to date.[17] At the same time, it represents the first discrete POM with a paramagnetic core and shell, and it can also be viewed as a hybrid polyoxoanion/coordination complex.

The core of polyanion **1** (see Figure 3) is most closely related to Weakley's trimeric tungstophosphate $[Co_9(OH)_3(H_2O)_6(HPO_4)_2(PW_9O_{34})_3]^{16-}$.[18] However, in this species the three Keggin tungsten-oxo fragments are of the (*B*-α-PW_9O_{34}) type, and the central nonacobalt cluster is capped by a HPO_4^{2-} ligand above and below. The magnetic properties of $[Co_9(OH)_3(H_2O)_6(HPO_4)_2(PW_9O_{34})_3]^{16-}$ have been investigated thoroughly by Coronado and co-workers.[19]

Bond valence sum calculations (BVS) on **1** indicate that all terminal ligands associated with Co^{II} ions are water molecules (6 associated with the Co_9 core and 30 with the outer Co-antenna).[20] Furthermore, the three μ_3-oxo within

(14) (a) Casañ-Pastor, N.; Bas-Serra, J.; Coronado, E.; Pourroy, G.; Baker, L. C. W. *J. Am. Chem. Soc.* **1992**, *114*, 10380. (b) Gómez-García, C. J.; Coronado, E.; Borrás-Almenar, J. J. *Inorg. Chem.* **1992**, *31*, 1667.
(15) (a) Cage, B.; Hassan, A. K.; Pardi, L.; Krzystek, J.; Brunel, L. C.; Dalal, N. S. *J. Magn. Reson.* **1997**, *124*, 495. (b) Hassan, A. K.; Pardi, L. A.; Krzystek, J.; Sienkiewicz, A.; Goy, P.; Rohrer, M.; Brunel, L. C. *J. Magn. Reson.* **2000**, *142*, 300.
(16) Laronze, N.; Marrot, J.; Hervé, G. *Inorg. Chem.* **2003**, *42*, 5857.
(17) Mialane, P.; Dolbecq, A.; Marrot, J.; Rivière, E.; Sécheresse, F. *Angew. Chem., Int. Ed.* **2003**, *42*, 3523.
(18) Weakley, T. J. R. *J. Chem. Soc. Chem. Commun.* **1984**, 1406.
(19) Galán-Mascarós, J. R.; Gómez-García, C. J.; Borrás-Almenar, J. J.; Coronado, E. *Adv. Mater.* **1994**, *6*, 221.

the Co_9 core of **1** are hydroxo groups (see Figure 3). All of the above combined indicates a charge of −5 for **1**. We were able to locate only three sodium counterions by X-ray diffraction, most likely due to disorder. However, the presence of the remaining two sodium ions was established by elemental analysis.

As mentioned above, polyanion **1** is composed of three (β-SiW_8O_{31}) fragments and to our knowledge this fragment has never been observed before in polyoxoanion chemistry. However, very recently we isolated another cobalt-substituted tungstosilicate containing the same fragment.[21] We must remember that **1** was synthesized starting from [γ-$SiW_{10}O_{36}$]$^{8-}$. Therefore, the mechanism of formation of **1** must involve metal insertion, rotational isomerization (γ-Keggin → β-Keggin), and loss of tungsten (SiW_{10} → SiW_8). It is not clear if **1** is formed from three monomeric Keggin fragments in one condensation step or by gradual growth involving a dimeric intermediate. Furthermore, it is not clear at which point of formation of **1** the antenna-like, outer Co^{II} ions come into play. The detailed mechanism of formation of POMs (including the largest ones known) via self-assembly remains one of the mysteries in inorganic chemistry.

Electrochemistry. (a) Solubility and Stability. In NaCl media, **1** is very sparingly soluble at pH > 1 and that phenomenon is the more pronounced the higher is the pH. The solubility can be increased by replacing NaCl by LiCl. Furthermore, solubilization in these media is accompanied by an important proton consumption. For instance, addition of 0.2 mM **1** to 1 M LiCl + HCl (pH = 3) drives the final pH to 5.50. The initial pH must be lower than 2 if a negligible proton consumption is to be measured with 0.2 mM **1** in 1 M LiCl medium. As a consequence of these observations, buffers with a large capacity (like LiCl + potassium hydrogenophthalate + HCl) are necessary to avoid such important pH variations upon dissolution of **1**. These remarks are particularly important in electrochemistry and electrocatalysis with POMs where electron transfers are usually accompanied by acid−base equilibria. The results for **1** are reminiscent of the behavior described for [$P_8W_{48}O_{184}$]$^{40-}$, which has also several protonation sites.[22]

With the choice of appropriate media for the solubilization of **1**, it was possible to study its stability from pH 0 through 5 either by monitoring its UV/vis spectrum for at least 24 h or by voltammetry for about 10 h. Solutions of **1** give reproducible characteristics by these two techniques. These results suggest strongly **1** to be stable in solution from pH 0 to at least pH 5. In short, chloride media are necessary to ensure stability of **1**.

(b) Voltammetric Studies. Figure 4 shows the cyclic voltammogram of **1** in HCl medium (pH = 0.27). The potential domain will be divided in a positive and negative one (vs SCE), for a sequential description of observed phenomena. Before the water oxidation process in the positive potential domain, a redox couple was observed with

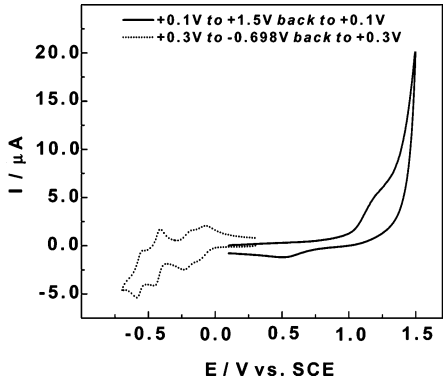

Figure 4. Cyclic voltammograms of a 2×10^{-4} M solution of **1** in HCl (pH = 0.27) medium; working electrode: glassy carbon; reference electrode: SCE; scan rate: 10 mV s^{-1}.

an oxidation peak located at +1.230 V vs SCE and the associated reduction at +0.50 V. This pattern is attributed to the redox processes of Co^{II} ions. This observation deserves emphasis: to the best of our knowledge, this is the first time that the oxidation of Co(II) in multi-cobalt POMs is detected. Only monosubstituted POMs and [$Co^{II}W_{12}O_{40}$]$^{6-}$ were previously described to display an electroactive Co center.[1,23] However, the voltammetric pattern is very unsymmetrical, with the cathodic branch much smaller than the anodic one. Probably, this phenomenon must be linked with a film deposition on the electrode surface during the anodic scan. This process was much faster when the pH of the supporting electrolyte was increased. It results in a current increase and a correlated increase of the electrode surface at every cycle. This observation precludes any reliable determination of the number of electrons involved in the Co^{II} redox processes.

The problem arises as to the identity of the Co^{II} centers actually participating in the redox processes. For this purpose, the CV of $CoCl_2$ was run in the same HCl medium. The concentration of $CoCl_2$ was selected with the hypothesis that the six external Co centers of **1** might be free in solution. Comparison of the CVs of **1** and $CoCl_2$ is enlightening. The striking observation is the large difference in current intensities. At 1.172 V vs SCE, which corresponds approximately to the respective peak potentials, the current intensity ratio is 3.3 in favor of the free Co^{II} ions. This difference suggests strongly that the satellite Co^{II} centers remain fixed on **1**, the diffusion coefficient of which is much smaller than that of free Co^{II} ions.

Reduction of the W(VI) centers in **1** is expected to occur in the negative potential domain. The CV in Figure 5 is restricted to the four reversible waves obtained in this area, with the reduction peak potentials in a pH 0.27 medium located at −0.128, −0.232, −0.454, and −0.584 V, respectively. To our knowledge, the peak potential of the first W-wave in the formerly unknown (β-SiW_8O_{31}) fragment is one of the least negative reported for POMs. For example, we note this wave to be more positive than that observed for the nickel-substituted species [$Ni_6As_3W_{24}O_{94}(H_2O)_2$]$^{17-}$

(20) Brown, I. D.; Altermatt, D. *Acta Crystallogr.* **1985**, *B41*, 244.
(21) Kortz et al. Manuscript in preparation.
(22) Keita, B.; Lu, Y. W.; Nadjo, L.; Contant, R. *Electrochem. Commun.* **2000**, *2*, 720.
(23) Keita, B.; Lu, Y. W.; Nadjo, L.; Contant, R.; Abbessi, M.; Canny, J.; Richet, M. *J. Electroanal Chem.* **1999**, *477*, 146 and references therein.

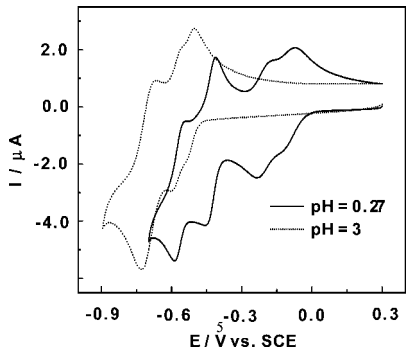

Figure 5. Cyclic voltammograms of a 2×10^{-4} M solution of **1** in two different pH media; working electrode: glassy carbon; reference electrode: SCE; scan rate: 10 mV s^{-1}. Full line: pH 0.27 (HCl); dotted line: pH 3 (1 M LiCl + HCl + 0.069 M PHP, adjusted to exactly pH 3).

and $[Ni_4Mn_2P_3W_{24}O_{94}(H_2O)_2]^{17-}$.[24] Controlled potential electrolyses were carried out for **1** at the potential locations of these waves. They yield, invariably, products with the characteristic blue color of reduced tungsten centers (heteropoly blues). Quantitatively, an electrolysis performed at −0.348 V in the pH 0.27 medium indicated that the first two very close waves correspond to the consumption of 4 electrons per molecule. Figure 5 shows the evolution of W-waves for **1** at pH 0.27 and pH 3, respectively. As expected, the W-waves shift in the negative potential direction when the pH of the electrolyte increases. However, the point worth noting is the extreme sensitivity of the W centers in the novel (β-SiW_8O_{31}) fragment to pH changes. This behavior must be attributed to the pK_a values of reduced intermediate of **1**. It is also recalled that for accurate control of pH > 1 values a careful choice of electrolyte composition is required. This may include, for example, addition of an appropriate amount of a proton donor like potassium hydrogen phthalate (PHP) to the electrolyte.[22] In the potential domain explored for **1**, the number of waves and also the number of electrons corresponding to each wave are pH-dependent.

Magnetic Studies. Figure 6a displays the results of the magnetic measurements on **Na_5-1**. The effective moment $\chi_m T$ decreases continuously with decreasing temperature, showing the presence of antiferromagnetic exchange interactions. When we compare the experimental 300 K $\chi_m T$ value of ~43 emu K/mol (~ 18.5 μ_B) to that of the spin only value of 28.13 emu K/mol (15 μ_B) for 15 non-interacting Co^{II} ions ($S = 3/2$) with $g = 2.0$, we can see that there is an appreciable spin−orbit coupling, which is expected for octahedrally coordinated Co^{II} ions.[25]

Figures 1 and 2 show that 6 out of 15 Co^{II} ions are present on the periphery of the molecule, far from each other (~7.7 Å) and also far (~6.6 Å) from the core of 9 Co^{II} ions. Thus the entire system of 15 Co^{II} ions can therefore be considered essentially as two independent subsystems. In our analysis, we neglected both of these spin exchange interactions and

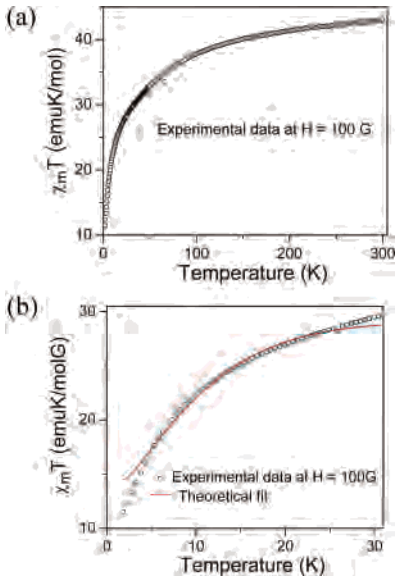

Figure 6. (a) Temperature dependence of $\chi_m T$ for $Na_5[Co_6(H_2O)_{30}\{Co_9Cl_2(OH)_3(H_2O)_9(\beta\text{-}SiW_8O_{31})_3\}]\cdot 37H_2O$ (**Na_5-1**). (b) Theoretical fit to the experimental data in the temperature range 1.8−30 K.

considered the contribution of the 6 peripheral Co^{II} ions to the total magnetic moment as additive.

The 9 exchange-coupled Co^{II} ions in the core of **1** can be viewed as three triangular units belonging to three Keggin fragments that are connected by two chloro bridges (see Figure 3). To explain the observed magnetic properties of **Na_5-1**, we made the following assumptions:

(1) Each $(Co^{II})_3$ triangle is considered as equilateral, neglecting the small difference between Co_1-Co_{1a} (3.037 Å) and $Co_{1(1a)}-Co_2$ distances (3.141 Å), see Figure 3. (2) The total magnetic susceptibility is taken as a sum of the $(Co^{II})_9$ core and the six uncoupled peripheral Co^{II} ions with effective spin $S = 1/2$. (3) Since the bond angles and bond lengths of our $(Co^{II})_9$ core are very similar to that in $[Co_9(OH)_3(H_2O)_6(HPO_4)_2(PW_9O_{34})_3]^{16-}$, the fully anisotropic Ising model described by Coronado and co-workers has been employed.[19]

As in ref 19, we restrict our analysis to the low temperature (T < 30 K) range, where only the lowest lying Kramer's doublet with effective spin $S = 1/2$ is populated. Following ref 26, we see that the direct product of nine representations of the rotation group of symmetry $D_{1/2}$ corresponding to the central nine Co^{II} ions is $D_{1/2} \otimes D_{1/2} \otimes D_{1/2} \otimes D_{1/2} \otimes D_{1/2} \otimes D_{1/2} \otimes D_{1/2} \otimes D_{1/2} \otimes D_{1/2} = 42D_{1/2} \oplus 48D_{3/2} \oplus 27D_{5/2} \oplus 8D_{7/2} \oplus D_{9/2}$, giving rise to 126 spin states. Assumption 1 (approximation of equilateral triangle) reduces these energy levels to 14 distinct ones (see Table 2). The appropriate spin exchange Hamiltonian can then be written as:[19]

$$\hat{H}_{ex,core} = -2J_{1Z}[\hat{S}_{1Z}\hat{S}_{3Z} + \hat{S}_{1Z}\hat{S}_{2Z} + \hat{S}_{2Z}\hat{S}_{3Z} + \hat{S}_{4Z}\hat{S}_{5Z} + \hat{S}_{4Z}\hat{S}_{5Z} + \hat{S}_{5Z}\hat{S}_{6Z} + \hat{S}_{7Z}\hat{S}_{9Z} + \hat{S}_{7Z}\hat{S}_{8Z} + \hat{S}_{8Z}\hat{S}_{9Z}] - 2J_{2Z}[\hat{S}_{1Z}\hat{S}_{4Z} + \hat{S}_{1Z}\hat{S}_{7Z} + \hat{S}_{4Z}\hat{S}_{7Z} + \hat{S}_{2Z}\hat{S}_{5Z} + \hat{S}_{2Z}\hat{S}_{8Z} + \hat{S}_{5Z}\hat{S}_{8Z}] \quad (1)$$

where J_{1Z}, J_{2Z} correspond to the Z-component of intra- and inter-trimer spin exchange interactions, respectively, and $\hat{S}_{iZ}$

(24) Mbomekalle, I. M.; Keita, B.; Nierlich, M.; Kortz, U.; Berthet, P.; Nadjo, L. *Inorg. Chem.* **2003**, *42*, 5143.
(25) (a) Carlin, R. L. *Magnetochemistry*; Springer-Verlag: New York, 1983. (b) Kahn, O. *Molecular Magnetism*; VCH: New York, 1993.

Table 2. Spin Energy Levels of $[Co_6(H_2O)_{30}\{Co_9Cl_2(OH)_3(H_2O)_9(\beta\text{-}SiW_8O_{31})_3\}]^{5-}$ (**1**) Corresponding to Different Intermediate Spins S_{123}, S_{456}, and S_{789}[a]

S_T	$E(S_T, S_{123}, S_{456}, S_{789})$
9/2	$-4.5J_{1Z} - 13.5J_{2Z}$
7/2	$-1.5J_{1Z} - 7.5J_{2Z}$
7/2	$-4.5J_{1Z} - 4.5J_{2Z}$
5/2	$1.5J_{1Z} - 3.5J_{2Z}$
5/2	$-1.5J_{1Z} - 0.5J_{2Z}$
5/2	$-4.5J_{1Z} + 2.5J_{2Z}$
3/2	$4.5J_{1Z} - 1.5J_{2Z}$
3/2	$1.5J_{1Z} + 1.5J_{2Z}$
3/2	$-1.5J_{1Z} + 4.5J_{2Z}$
3/2	$-4.5J_{1Z} + 7.5J_{2Z}$
1/2	$4.5J_{1Z} + 1.5J_{2Z}$
1/2	$1.5J_{1Z} + 4.5J_{2Z}$
1/2	$-1.5J_{1Z} + 7.5J_{2Z}$
1/2	$-4.5J_{1Z} + 10.5J_{2Z}$

[a] See text for details.

is the *Z*-component of the spin operator associated with the effective spin $S = 1/2$ of the *i*th atom. The numbering of the atoms in eq 1 from 1−9 corresponds to the cobalt ions 1, 1a, 2, 1′, 1a′, 2′, 1″, 1a″, and 2″, respectively (see Figure 3). The eigenvalues corresponding to eq 1 are given in eq 2:

$$E(S_T, S_{123}, S_{456}, S_{789}, S_1, S_2, S_3, S_4, S_5, S_6, S_7, S_8, S_9) = -J_{1Z}[S_{123}(S_{123}+1) + S_{456}(S_{456}+1) + S_{789}(S_{789}+1) - S_1(S_1+1) - S_2(S_2+1) - S_3(S_3+1) - S_4(S_4+1) - S_5(S_5+1) - S_6(S_6+1) - S_7(S_7+1) - S_8(S_8+1) - S_9(S_9+1)] - J_{2Z}[S_T(S_T+1) - S_{123}(S_{123}+1) - S_{456}(S_{456}+1) - S_{789}(S_{789}+1)] \quad (2)$$

For effective spin $S_i = 1/2$, eq 2 can be rewritten as (eq 3):

$$E(S_T, S_{123}, S_{456}, S_{789}) = -J_{1Z}[S_{123}(S_{123}+1) + S_{456}(S_{456}+1) + S_{789}(S_{789}+1) - 27/4] - J_{2Z}[S_T(S_T+1) - S_{123}(S_{123}+1) - S_{456}(S_{456}+1) - S_{789}(S_{789}+1)] \quad (3)$$

The experimental $\chi_m T$ data were fit (see Figure 6b) to the parallel magnetic susceptibility expression given in eq 4:

$$(\chi_m T)_{para} = (\chi_m T)_{core,para} + 6Ng^2\beta^2S(S+1)/3k \quad (4)$$

where *N* is the Avogadro number, *g* is the Landé *g*-factor, β is the electron Bohr magneton, and *k* is the Boltzmann constant. In eq 4, the first term corresponds to the nine central Co^{II} ions whereas the second term represents the contribution from the six peripheral Co^{II} ions with effective spin $S = 1/2$. The expression for $(\chi_m T)_{core,para}$ can be derived (cf. eq 5) using the HDVV equation[25] and the energies listed in Table 2:

$$(\chi_m T)_{core,para} = \left(\frac{Ng^2\beta^2}{k}\right)\left(\frac{A}{B}\right) \quad (5)$$

where *N*, *g*, β, and *k* have their usual meaning and $A = 165 + 504\exp(3x + 6y) + 168\exp(9y) + 420\exp(6x + 10y) + 420\exp(3x + 13y) + 210\exp(16y) + 80\exp(9x + 12y) + 240\exp(6x + 15y) + 120\exp(3x + 18y) + 40\exp(21y) + 16\exp(9x + 15y) + 12\exp(6x + 18y) + 12\exp(3x + 21y) + 2\exp(24y)$, $B = 5 + 24\exp(3x + 6y) + 8\exp(9y) + 36\exp(6x + 10y) + 36\exp(3x + 13y) + 9\exp(16y) + 16\exp(9x + 12y) + 48\exp(6x + 15y) + 24\exp(3x + 18y) + 8\exp(21y) + 16\exp(9x + 15y) + 12\exp(6x + 18y) + 12\exp(3x + 21y) + 2\exp(24y)$ with $x = J_{1Z}/kT$ and $y = J_{2Z}/kT$. The best-fit values are $J_{1Z} = 17.0 \pm 1.5$ cm^{-1}, $J_{2Z} = -13 \pm 1$ cm^{-1}, and $g = 2.42 \pm 0.01$. This *g* value is about the same as those reported for other high spin octahedral Co^{II} ions.[26] We note that while the fit is not as satisfactory as it could be, the analysis clearly showed that the intra-trimer interactions are ferromagnetic while the inter-trimer interactions are antiferromagnetic. The spin exchange parameters are in good agreement with the values reported in the literature for $[Co_4(H_2O)_2(PW_9O_{34})_2]^{10-}$ (ref 14) and $[Co_9(OH)_3(H_2O)_6(HPO_4)_2(PW_9O_{34})_3]^{16-}$ (ref 19).

The signs and relative magnitudes of the exchange parameters J_{1Z} and J_{2Z} correlate reasonably well with the structural features of **1**. The intra-trimer Co−O−Co angles are in the range 94−101° favoring orthogonality of the magnetic orbitals. Therefore, ferromagnetic spin exchange interactions are expected. On the other hand, the Co−Cl−Co angles (∼119°) are significantly larger, suggesting the presence of antiferromagnetic interactions between trimers. Also, the average Co−Co intra-trimer distances (3.1 Å) are much shorter than the inter-trimer distances (4.3 Å). As a result, we expect the magnitude of intra-trimer exchange interactions to be stronger than that of inter-trimer exchange.

Electron Paramagnetic Resonance Studies. The magnetization data were complemented by powder EPR measurements over a wide frequency and temperature range. Figure 7 shows the 4 K EPR spectrum of **Na_5-1** at 34 and 93 GHz, respectively. There is a broad, asymmetric transition at low field, associated with an anisotropic Kramer's doublet.[26] The small peak at $g \approx 2$, marked as "A" in Figure 7, is due to an impurity most likely a result of air oxidation but is not of interest here because of its small concentration. The effective *g* values associated with the Kramer's doublet are $g_{eff}(xx) = 2.63$, $g_{eff}(yy) = 3.89$, and $g_{eff}(zz) = 5.72$, as expected for Co^{II} systems.[26,27] The EPR spectra for **Na_5-1** are quite similar to those reported by Coronado et al. for $[Co_4(H_2O)_2(PW_9O_{34})_2]^{10-}$ and $[Co_9(OH)_3(H_2O)_6(HPO_4)_2(PW_9O_{34})_3]^{16-}$ and thus our effective *g*-values are also in agreement.[14,19,27] This effective $S = 1/2$ ground state is in agreement with the magnetic susceptibility analysis. For **Na_5-1** we observed no other transitions up to 400 GHz, and so we tentatively concluded that the zero-field splitting parameter (*D*) is much larger than 400 GHz (∼14 cm^{-1}). This interpretation is consistent with literature data on related Co-substituted polyoxoanions.[14,19] As the temperature is

(26) Abragam, A.; Bleaney, B. *Electron Paramagnetic Resonance of Transition Ions*; Dover Publications: New York, 1970.

(27) (a) Andres, H.; Clemente-Juan, J. M.; Aebersold, M.; Güdel, H. U.; Coronado, E.; Büttner, H.; Kearly, G.; Melero, J.; Burriel, R. *J. Am. Chem. Soc.* **1999**, *121*, 10028. (b) Andres, H.; Clemente-Juan, J. M.; Basler, R.; Aebersold, M.; Güdel, H. U.; Borrás-Almenar, J. J.; Gaita, A.; Coronado, E.; Büttner, H.; Janssen, S. *Inorg. Chem.* **2001**, *40*, 1943. (c) Clemente-Juan, J. M.; Coronado, E.; Gaita-Ariño, A.; Giménez-Saiz, C.; Chaboussant, G.; Güdel, H. U.; Burriel, R.; Mutka, H. *Chem. Eur. J.* **2002**, *8*, 5701.

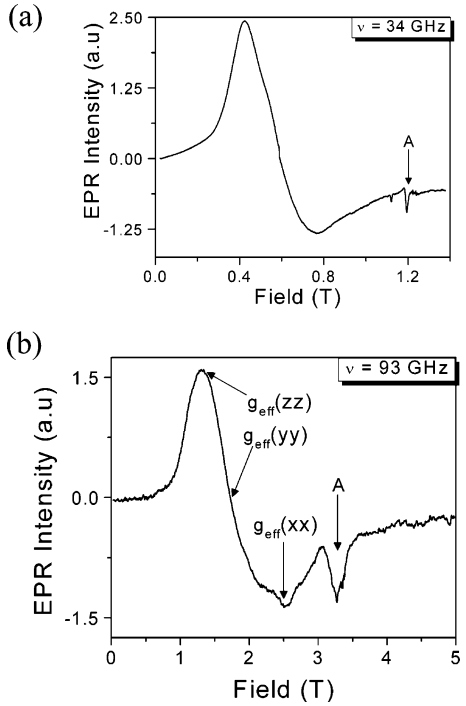

Figure 7. (a) Q-band (34 GHz) and (b) W-band (93 GHz) EPR spectra for **Na_5-1** at 4 K. "A" denotes an unassigned resonance that we ascribe to be from an impurity. See text for details.

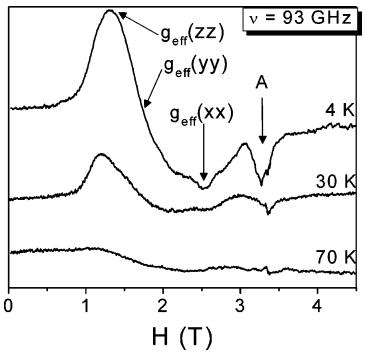

Figure 8. Temperature dependence of **Na_5-1** at 93 GHz. "A" corresponds to an impurity peak shown in Figure 7.

increased, the EPR signal intensity decreases and becomes undetectable above 70 K (see Figure 8), most likely due to line broadening from fast spin−lattice relaxation processes.

Conclusions

The 15-cobalt-substituted polyoxotungstate $[Co_6(H_2O)_{30}\{Co_9Cl_2(OH)_3(H_2O)_9(\beta\text{-}SiW_8O_{31})_3\}]^{5-}$ (**1**) has been synthesized by interaction of Co^{II} ions with the dilacunary $[\gamma\text{-}SiW_{10}O_{36}]^{8-}$ in a simple one-pot procedure in aqueous, acidic NaCl medium. The trimeric **1** has a core of nine Co^{II} ions encapsulated by three unprecedented (β-SiW_8O_{31}) fragments and two Cl^- ligands. This assembly is surrounded by six antenna-like $Co^{II}(H_2O)_5$ groups resulting in the satellite-like structure **1**. Polyanion **1** represents only the second example of a structurally characterized cobalt-substituted tungstosilicate. Furthermore, **1** contains more paramagnetic transition metal centers than any other polyoxotungstate known to date. We believe that the six $Co^{II}(H_2O)_5$ antenna allow for incorporation of a variety of mono-, di-, and tridentate ligands leading to derivatives with interesting properties. Furthermore, it can be envisioned to substitute the six external cobalt ions by other paramagnetic as well as diamagnetic ions, resulting in isostructural polyanions with different redox and magnetic properties. Therefore, we believe that **1** is the parent compound of a novel and important subclass of transition metal substituted polyoxotungstates.

Cyclic voltammetry of **1** was studied as a function of pH. Comparison of the current intensities for redox processes of the Co^{II} centers of **1** with free Co^{II} ions in solution suggests strongly that the six outer Co^{II} ions remain attached to **1** in solution. The electrochemical properties of **1** allow to envision further investigations, starting with the search for appropriate solvent media for facile handling of **1**. Finally, the anticipated stability of **1** in these media will allow for detailed studies of its electrochemical and catalytic properties. Magnetic studies of **Na_5-1** reveal the presence of both ferromagnetic intra-trimer interactions and antiferromagnetic inter-trimer interactions for the Co_9 core.

Acknowledgment. This work was supported by the International University Bremen, the CNRS (UMR 8000), and the University Paris-Sud XI. Florida State University would like to thank the National Science Foundation (NIRT), DMR 0103290, for support. Figures 1−3 were generated by Diamond Version 2.1e (copyright Crystal Impact GbR).

Supporting Information Available: Complete X-ray crystallographic data for **Na_5-1** (CIF format). This material is available free of charge via the Internet at http://pubs.acs.org.

IC048269X